Anomalous Diffusion of Adsorbed Water
A Neutron Scattering Study of Hydrated Myoglobin *

Faraday Discussion 103 (1996) 269-280
M. Settles and W. Doster†
Technische Universität München
Physik-Department E13, D-85747 Garching, Germany

Abstract

The neutron scattering spectrum of bound H_2O was determined from the excess scattering of H_2O-hydrated myoglobin relative to a sample hydrated with D_2O. The resulting vibrational difference spectrum shows the well known translational and librational bands of bulk water. Significant discrepancies arise at low frequencies indicating that the diffusive motion is strongly retarded by interactions with the protein surface. By Fourier deconvolution of constant Q-spectra we obtain the intermediate scattering function and the time resolved mean square displacement of the water protons on a 15 ps time scale. We observe a sublinear increase in the squared displacements with time suggesting anomalous diffusion. Furthermore, the fourth moment $\langle r^4(t)\rangle$ exceeds the value expected for a Gaussian distribution, which indicates either strong heterogeneity or anisotropic motions. The data are discussed in relation to simulations and theoretical results on strongly coupled liquids.

*to be published in: FARADAY DISCUSSION No: 103, ROYAL SOCIETY OF CHEMISTRY, 1996: Hydration Processes in Biological and Macromolecular Systems

†To whom correspondence should be addressed: wolfgang.doster@physik.tu-muenchen.de

1. Introduction

The properties of water molecules interacting with a protein surface differ from those in the bulk phase. The perturbation must be substantial since crystallization is suppressed at least for the first two layers. Hydration water can thus be supercooled easily and freezes forming a glass below 180 K [1, 2]. Bulk water is known to form transient, ordered patches of low density in which the molecules are hydrogen-bonded to four neighbours. Order fluctuations of the patch size account for the well known anomalies in the second derivatives of the free energy of water. Furthermore, hydrogen bonds connecting water to charged and polar surfaces are thought to act as patch breakers, while nonpolar interactions enhance the formation of short range order [3]. The dominance of patch breaking may explain why hydration water does not crystallize. These structural effects [4] have their counterpart in changes in mobility: Dielectric relaxation spectroscopy and n.m.r. determine rotational correlation times of 70 - 80 ps compared to 8 ps in the bulk. A similar ratio was reported for translational diffusion [5, 6, 7, 8]. The depression in mobility reflects the constraints imposed by hydrogen bonding of water to protein residues which are in general quite rigid. The question of how water displacements couple to protein structural motions and how this contributes to biological activity is still open. Of primary relevance are those fluctuations which involve changes in hydration, such as folding or substrate binding. These processes depend on the residence times of water molecules near the protein surface. The exchange takes place within 300 ps as was shown for trypsin inhibitor in solution [9].
However protein-water correlations also involve much shorter times: Molecular dynamic simulations [10, 11, 12] and neutron scattering experiments[13] on partially hydrated myoglobin and other proteins reveal fast structural relaxation processes which depend on hydration water:
The mean square displacements of hydrogens in the solvated protein display a striking nonlinear increase with temperature above 180 K, while harmonic, linear behaviour is found at low temperatures. Time resolved analysis shows that diffusive modes appear in parallel on a 10 ps time scale and above. The anharmonic protein motions can be suppressed by dehydration [14, 15, 11, 16]. This suggests that the dynamical contribution of water to protein flexibility arises within a few picoseconds. Above ≈70 ps, the ro-

tational correlation time of bound water, this influence reduces to viscous damping. In this study we focus on fast water displacements on a time scale below 20 ps.

Inelastic neutron scattering proved to be a very useful tool to measure ensemble averaged water trajectories. The incoherent scattering by the water protons reveals the tagged particle displacements. Extensive studies have been performed on perdeuterated phycocyanin[17] and bacteriorhodopsin [18, 19]. Perdeuteration suppresses the background of protein protons, since the cross section of ^{2}H is small compared to ^{1}H. In the case of native purple membrane a difference method was employed using H_2O/D_2O exchange [19]. The neutron scattering spectrum in these studies was modelled by jump diffusion in analogy to previous investigations on bulk water [20, 21]. However, the resulting parameter values are somewhat puzzling: In the case of phycocyanin the mobile water fraction is assumed to perform confined translational diffusion within a sphere of diameter 6 Å. The authors obtain a diffusion coefficient in the sphere close to bulk water results. But the residence time between successive jumps is about four times larger (4 ps at 293 K) and implies a factor of two larger jump length in spite of confinement [17, 22]. In the case of hydrated purple membrane a jump time of even 70 ps has been derived [18]. Furthermore, the associated proton jump length of 4.1 Å is also significantly larger than in the bulk. In contrast, the deduced rotational correlation time of 10 ps approaches the bulk water value in disagreement with results mentioned above.

Where do these differences come from? It is not clear how much the parameter values depend on the assumptions used to model the data. For instance, it is not clear whether the decoupling approximation which allows to separate translation from rotation, applies to bound water. To avoid these problems we prefer the alternative approach which consists in a model independent analysis. The feasibility will be demonstrated below. For the first time we determine the intermediate scattering function and the time resolved mean square displacements of hydration water based on a general method. These results will be compared with bulk water data [23, 24], computer simulations [25] and mode coupling theory of simple liquids [26].

We investigate horse-myoglobin hydrated with H_2O and D_2O to $h = 0.35$ g/g. The corresponding number of water molecules ≈ 350 is sufficient to cover the entire protein surface. To simplify the situation we are not including a bulk water phase, which avoids exchange between phases and ice formation. We

have shown that this hydration is sufficient to initiate anharmonic protein flexibility above 180 K [13, 27]. As a functional control, we studied ligand bindig to partially hydrated myoglobin using flash photolysis [28]. The most significant effect of dehydration consists in reducing the ligand exchange rate between heme pocket and the surface. However, at 0.35 g/g the rate is still within 30% of the value observed in solution. Since 1975 myoglobin has been one of the most important model systems to study the connection of protein-dynamics and function [29]. For this molecule the puzzling result was obtained that water reorientation and fluctuations of the heme group display a common temperature dependence in spite of a factor 100 difference in time scales [30].

2. Materials and Methods

Hydrated samples of horse myoglobin (Mb, Sigma) were obtained by rehydrating lyophilized material with H_2O or D_2O in a controlled humidity environment. The degree of hydration was determined by weighing. A typical amount of 300-500 mg of sample was held in a thin walled vacuum tight aluminium cell of diameter 50 mm and 1.5 mm intervall spacing. The samples were measured using the time-of-flight spectrometer IN6 (ILL, Grenoble) at a wavelength of 5.1 Å and oriented at 135° to the incident beam. The transmission was close to 0.9. To obtain data of sufficient quality required 6 to 8 hours of beam time per sample and temperature. The initial data reduction was performed using standard ILL programs which correct for incident flux, cell scattering and self shielding using an angle dependent slab correction. To compensate for detector efficiency the data were normalized with a vanadium spectrum.
The scattering function was measured versus scattering angle θ and energy exchange $\hbar\omega$: $S(\theta, \omega)$. To derive the dynamical structure factor, S(Q,ω), ($\hbar$Q denotes the momentum exchange) the data are transformed into a constant Q format using an interpolation procedure [31]. This step is essential since the scattering vector Q varies with ω at fixed scattering angle because of the neutron kinematics.

The dynamics of hydration water was determined from the excess scattering

of H_2O-hydrated myoglobin relative to the D_2O-hydrated protein. As the spectra are dominated by the incoherent scattering from the protons, the following numbers were used for proper normalisation of the data:

type of proton	H_2O hydrated	D_2O hydrated
carbon bound, not exchangeable	≈ 1000	≈ 1000
surface bound, exchangeable	≈ 130	-
amide protons, exchange dependent		
on exposure time to D_2O	≈ 150	75 ± 25
water	700...750	-
sum	≈ 2000	$\approx 1050...1100$

The fraction f_P of protein protons to be subtracted thus amounts to 50-55 %, given that the individual spectra are properly normalised. For normalisation of the data we use the frequency integral $\int S(Q,\omega)d\omega$ at fixed wavevector Q. The resulting normalisation function $N_P(Q,T)$ was independent of temperature within 2 %, but shows variations with Q due to the residual 10 % coherent contribution to the mainly incoherent signal. The structure factor of hydration water is then calculated from:

$$S_{hydr.w.}(Q,\hbar\omega) = \frac{S_{P+H_2O}(Q,\hbar\omega) - f_P \cdot S_{P+D_2O}(Q,\hbar\omega)}{1 - f_P}\,. \qquad (1)$$

The resulting spectra contain an approximate 20 % contribution from exchangeable protein protons. To estimate the relevance of this effect we consider two limiting cases. Case I: The exchangeable hydrogens are dynamically equivalent to water protons. Case II: The labile hydrogens move like the nonexchangeable protons. Experiments performed with protonated and D-exchanged protein at low hydration allow to exclude a kinetic isotope effect on protein motions. The D-exchange did not modify the spectral lineshape. To a first approximation, exchange only affects the scale factor f_P of the protein background [32]. Unless specified otherwise we assume case I.

The Q-dependence at constant energy transfer was parametrized as a polynomial in Q^2, appropriate for incoherent scattering from isotropic samples:

$$S(Q,\omega) = A(\omega) + B(\omega) \cdot Q^2 + C(\omega) \cdot Q^4 \qquad (2)$$

For incoherent scattering from a perfectly harmonic system this is just the Placzek expansion with the offset A(ω) taking into account multiple scattering. We could reproduce the experimental offset quantitatively by calculating the double scattering intensities of the kind elastic-inelastic and inelastic-elastic. The calculations also show that this background is essentially Q-independent as assumed in the polynomial ansatz. The data were corrected for multiple scattering but the details will be discussed in ref. [31].

3. Vibrational Spectra: Dynamical Susceptibility

Fig. 1 compares selected spectra of hydration water with bulk water data: The figure shows the dynamical susceptibility, S(Q,ω)/n(ω,T). The normalisation of S(Q,ω) by the Bose occupation factor, n(ω,T), removes the temperature dependence in the one phonon approximation provided that the system is harmonic. The low frequency susceptibility of bulk water exhibits four distinct maxima [33, 34, 24]: the librational peak near 70 meV, two translational peaks, TA_1(7 meV) and TA_2 (22 meV) and the α-resonance, below 3 meV, which corresponds to diffusive structural relaxation. Fig. 1 combines neutron scattering [23] with depolarized light scattering experiments [24]. TA_2 involves only small proton displacements and is thus difficult to observe by neutron scattering. However, by superimposing neutron and light scattering data below 10 meV we found agreement almost within the error bars (not shown). This suggests that depolarized light scattering, in spite of Q$\approx 10^{-3}$Å^{-1} couples to the same microscopic motions that are seen at Q ≈ 2 Å^{-1} by neutron scattering [35]. At 270 K, as shown in fig. 1, the α-resonance has moved to lower frequencies and is now better resolved from the translational peak than at 300 K. The hydration water exhibits the same vibrational bands as bulk water with minor changes in frequency and intensity. However the α-resonance is missing. Instead one observes a deep minimum in the susceptibility. Note the steep increase below 0.2 meV which results from elastic scattering due to slow motions that are not resolved by the spectrometer. This observation clearly demonstrates that protein-water interactions slow down the structural relaxation of water substantially. The

low frequency spectrum of bulk water as shown in fig. 1 is complete and accounts entirely for macroscopic properties such as viscosity. The bound water spectrum in contrast is incomplete and exhibits only vibrational and local diffusive motions. The existence of local diffusive motions can be inferred from the strong temperature dependence of the susceptibility minimum (fig. 1). Therefore the effect of water on fast density fluctuations in the protein structure cannot simply be characterised by a microviscosity constant. Heterogeneity in time and space will play an important role. To get more insight into fast diffusive displacements of bound water we first transform the spectra to the time domain which yields the self-intermediate scattering function I(Q,t).

4. Diffusive Motions: Intermediate Scattering Function

Hydration water can be supercooled easily and turns into a glass below 180 K [1, 2]. In parallel the minimum in the susceptibility decreases and shifts to lower frequencies as shown in fig 1. The temperature dependence of the spectrum will be discussed elsewhere [31]. In the following we focus on high temperatures in search of translational diffusion.
To this end, the data at constant Q were Fourier deconvoluted from the instrumental resolution function in the time domain and corrected for multiple scattering. The resulting set of incoherent intermediate scattering functions I(Q,t) at 320 K is shown in fig. 2:
The two-step decay in the density correlations corresponds to dephasing of librational-translational modes and slow diffusive displacements respectively. In the hydrodynamic limit the translational self-diffusion implies a Gaussian incoherent scattering function:

$$I(Q,t) = f(Q) \cdot \exp\left(-t/\tau\right), \qquad Q \to 0 \tag{3}$$

with $1/\tau = \mathrm{D}\cdot \mathrm{Q}^2$ and f(Q) = 1 for Q→0. D denotes the translational diffusion coefficient and
1 - f(Q) represents the fraction of fast motions. Neutron scattering registers displacements on a microscopic scale or large Q. In the large Q-regime the

prediction of I(Q,t) is difficult because of the complexity of local interactions at short times. In the case of bound water, one can imagine a combined rotational- translational motion coupled to fast protein conformational changes. These interactions generally create some heterogeneity leading to nonexponential correlation functions. The observed time decay is indeed stretched and could be approximated by a Kohlrausch function:

$$I_K(Q,t) = f(Q) \cdot \exp\left(-(t/\tau_K)^{\beta}\right) \tag{4}$$

where β(Q)¡ 1 and τ_K(Q) depend on Q. The solid lines in fig. 2 represent two parameter fits (β, τ_K) of this function to the incoherent scattering data of bound water. The approximation appears reasonable at high Q and long times. At low Q unambiguous fits are not possible because of the small change in I(Q,t) in the accessible time window. The stretching parameter β varies between 0.3-0.4 as shown in fig. 3. The lineshape at large Q-values differs thus significantly from the Lorentzian case ($\beta = 1$) at small wavevectors. However, the average correlation time $\langle\tau_K(Q)\rangle$,

$$\langle\tau_K\rangle = \int dt\, I_K(Q,t)/f(Q) = \tau_K \cdot \Gamma(1/\beta)/\beta \tag{5}$$

shows approximately the same $1/\mathrm{Q}^2$ -dependence (fig. 3 and equ. 3) expected for small wavevectors. Assuming $1/\langle\tau_K\rangle = \mathrm{D}\cdot\mathrm{Q}^2$ we obtain an estimate of the long time diffusion coefficient D: For case I, we obtain $2\cdot10^{-7} cm^2/\mathrm{s}$, which is about a factor of 100 below the value of bulk water. In the opposite limit of case II, also shown in fig. 3, we find $0.01\,\mathrm{Å}^2/\mathrm{ps}$, still 20 times smaller than in the bulk. These results belong to the lower edge of published long time diffusion coefficients [6, 8], but at h = 0.35 g/g, we are investigating the primary shell of hydration.
The Q-dependence of $\langle\tau_K\rangle$ is regular but the fits of the data to equ.4 are incompatible with a Gaussian scattering law such as equ. 3: $(1/\tau^{\beta})$ is not proportional to Q^2. Non-Gaussian scattering could emerge for the following reasons: First, the distribution of dynamically accessible sites may be non-Gaussian. Second, the motion may be anisotropic. So even a Gaussian distribution along a particular coordinate will produce a non-Gaussian result after averaging over all orientations in an isotropic sample. A third possiblity could be an inhomogeneity in the displacement amplitudes.

The conclusions obtained so far are based on a phenomenological model, the Kohlrausch function. The model describes the long time behaviour rather well, but a precise test would require information at even longer times since $\langle \tau_K \rangle$ varies between 20 ps and 100 ps, which is outside of the experimental window. It is interesting in this context that quite similar results were derived recently in a neutron scattering study of glycerol, another glass-former where hydrogen bonds play a crucial role [36].
To get more insight into the short time and low Q behaviour, we now analyze the moments of the displacement distribution which does not involve any particular model.

5. Mean Square Displacements: Anomalous Diffusion

To evaluate the moments of I(Q,t), cuts at constant time are approximated by a polynomial up to second order in Q^2 which represents the Fourier transform of equ. 2:

$$I(Q,t) = A(t) + B(t) \cdot Q^2 + C(t) \cdot Q^4 \tag{6}$$

where A(t)$\equiv$ 1 in the ideal case of single scattering. For isotropic samples B(t) denotes the mean square displacement, B(t) = -$\frac{1}{6}\langle r^2(t) \rangle$. In the case of isotropic Gaussian scattering one has: C(t) = $\frac{1}{2}$ $B^2(t)$. C(t) is generally related to the fourth moment by: C(t) = $\frac{1}{120}\langle$ $r^4(t) \rangle$. Fig. 4 shows ln I(Q^2) at several instances of time together with the polynomial fits. The initial slope yields the second moment, the mean square displacement which increases with time. But in addition a nonzero curvature appears above 1 ps consistent with a non-Gaussian scattering profile. The corresponding deviation from a Gaussian displacement distribution can be quantified by the ratio C(t)/B^2(t). After correcting for multiple scattering the calculations converge to a ratio near 0.80 ($\pm$0.1) in excess of the Gaussian value of 0.5 as shown in fig. 5.

Fig. 6 finally shows the mean square displacements of bound water protons in comparison with a neutron scattering analysis of bulk water by Brockhouse

et al. [23] and molecular dynamic simulations [25]. Bulk water, both in the experiment and the simulation reaches the classical diffusion limit $\langle r^2(t)\rangle \propto$ t after $\approx$ 1 ps and $\approx$ 5 ps at 350 K and 300 K respectively. Hydration water in contrast shows no sign of a cross-over to normal diffusion on a 15 ps time scale even at the highest temperature of 320 K. Instead the displacements follow a power law: $\langle r^2\rangle \propto t^{0.4}$ at both temperatures. This result suggests that the displacement events are not homogeneously spread in time but occur in bursts. Such clusters may correlate with the simultaneous breaking of several hydrogen bonds. Thus, consistent with the Kohlrausch fit discussed above, we obtain a fractal time dependence in combination with a non-Gaussian displacement distribution.

6. Discussion

The understanding of the liquid state requires the knowledge of accurate time correlation functions [37]. This applies also to water in contact with a protein surface. Our main concern was to determine intermediate scattering functions of bound water without resorting to specific models. We find that the essential difference to bulk water consists in an extendend window of anomalous diffusion which opens between the vibrational and the hydrodynamic time scale. The anomaly reflects the coupling of water to protein residues. The interaction must include dynamic correlations, since a static distribution of diffusion coefficients, a reduction in dimensionality or stronger hydrogen bonding would not affect the linear time dependence of the squared displacements. Strong inter-particle correlations occur in supercooled liquids near a glass transition. Recent developments in mode coupling theory which account for this effect could reproduce the characteristic anomalies that are observed near the glass transition [38]. According to mode coupling theory the macroscopic viscosity reflects the dynamical constraints that a particle experiences in the microscopic cage formed by its nearest neighbours [38]. Approaching a critical density, the cage becomes a trap and the liquid appears structurally arrested on a macroscopic scale. The theory predicts certain universal results, which hold independently of the microscopic details. The theory was shown to applies to hard core liquids, where all dynamic properties can be derived using only the static structure factor as input [26].

But similar constraints seem to be relevant for softer potentials. The theory has been used to interpret experiments on various materials including the light scattering data of bulk water shown in fig.1 [24]. The protein surface, besides suppressing crystallization, seems to drive the water molecules towards a glassy state. To estimate the relevance of interparticle correlations we discuss our results in this general context. The data in fig. 1 display the high frequency wing of the α-relaxation. In this so-called von Schweidler regime, that is for times shorter than the structural relaxation time τ, the theory yields the following self-intermediate scattering function [39, 38]:

$$I(Q,t) = f(Q) - h_1(Q) \cdot (t/\tau)^b + h_2(Q) \cdot (t/\tau)^{2b} - ..., t \ll \tau \qquad (7)$$

Here the wavevector dependent coefficients f(Q, h_1(Q), h_2(Q) are solely determined by the equilibrium structure. The structural relaxation time, τ, reflects displacements on the scale of the interparticle distance and therefore, in contrast to τ_K, does not depend on Q. Both quantities should be identical for Q-values near the first maximum of the static structure factor. f(Q) denotes the strength of the α- relaxation as before and the h_i(Q) are called critical amplitudes. The von-Schweidler exponent, b, represents a characteristic quantity of the material and does not change with temperature. Expanding the Q-dependent factors for low Q and short times one obtains [39, 26]:

$$I(Q,t) \approx 1 - Q^2 r_s^2 - Q^2 \delta^2 (t/\tau)^b + ... \qquad (8)$$

r_s denotes the fast local displacements, while δ is associated with the escape out of the cage. For hard spheres these parameters are linked to the diameter a: $r_s \approx \frac{a}{9}$ and $\delta \approx \frac{a}{6}$[26]. The mean square displacement describing the inital phase of escape out of the cage is then given by:

$$\frac{1}{6}\langle r^2(t)\rangle \quad \approx \quad r_s^2 + \delta^2 \cdot (t/\tau)^b + O((t/\tau)^{2b}) \qquad (9)$$

The numerical values can be evaluated if the various partial structure factors of the liquid are known. A detailed discussion has been given for the hard sphere system [26, 40]. Equation (9) seems to be closely related to what we observe in fig. 6. Fitting the data at 320 K, we derive an effective

hard core diameter of bound water, a = 2.7(±0.1)Å, remarkably close the O–O distance of bulk water. For the exponent we get, b = 0.55(±0.05), the theoretical result for the hard-sphere liquid is 0.532 [26]. The relaxation time τ amounts to 5(±1) ps, five times larger than for bulk water [21]. The relaxation time should be compared with $\tau_K(Q = Q_{max})$ in fig. 3 which is about 10 ps for Q_{max} = 2 Å^{-1} in case I or 5 ps in case II. Since $\langle r^2(t)\rangle$ at short times does not depend significantly on how we treat the exchangeable protons, a consistency argument concerning τ would faviour case II over case I. The numbers are thus quite reasonable. However the small value of τ requires to complement the series in equs. (8,9) by further terms which leads to the intermediate Q and time regime. The experimental I(Q,t) in this range was approximated by a Kohlrausch function (equ. 3 and fig. 2). This result is again consistent with theoretical expectations: By solving the mode coupling equations numerically it was shown, that the Kohlrausch law can serve as an appropriate but not exact fitting function [38, 26]. It fails at short times and small Q which specifies the von-Schweidler regime. It is reassuring that the Kohlrausch fits to the calculated I(Q,t) yield an average correlation time (equ. 5) which varies with $1/Q^2$ even at large Q as in fig. 3. Although the interaction potential of water is badly approximated by a hard core the results discussed above suggest that the dynamic correlations induced by the cage effect and not the detailed nature of the constraints control the diffusive dynamics of bound water at short times. We finally mention that similar anomalies were oberved for the fluctuations of the protein structure on the same time scale [13, 41].

Acknowledgement: This work was financed in part by the Bundesministerium für Bildung und Forschung. We thank the ILL in Grenoble for excellent experimental support. We are also grateful for the various significant contributions of S. Cusack, F. Parak, W. Petry to this work.

Figure Captions:

Fig. 1: Dynamical susceptibility of bulk water (small symbols) and of hydration water (large symbols): broken line represents corrected neutron scattering data * [23], and the solid line denotes the light scattering results ** [24], circles: hydration water at 300 K and triangles: 180 K.

Fig. 2: Intermediate Scattering function of hydration water at 320 K assuming the exchangeable protons to be dynamically equivalent to water protons, case I. The lines represent fits to equ.4 assuming I(Q,0) = 1.

Fig. 3: The parameters of fitting the data to equ. 4, shown in fig.2: open symbols: case I and closed symbols: case II. The stretching parameter β, diamonds, the correlation time τ_K, circles and the average correlation time $\langle\tau_K\rangle$, triangles

Fig. 4: Intermediate scattering function ln I(Q,t) at fixed time points versus Q^2, showing that slope and curvature increase with time.

Fig. 5: The curvature of the data in fig. 4 corresponding to the fourth moment, normalized by the square of the second moment: the time evolution of $C(t)/B^2(t)$ in comparison with the Gaussian expectation.

Fig. 6: The time resolved x-mean square displacements of bulk water: neutron scattering, solid triangles **[23] and simulation, solid line * [25]. Hydration water at 300 and 320 K, solid circles and open triangles.

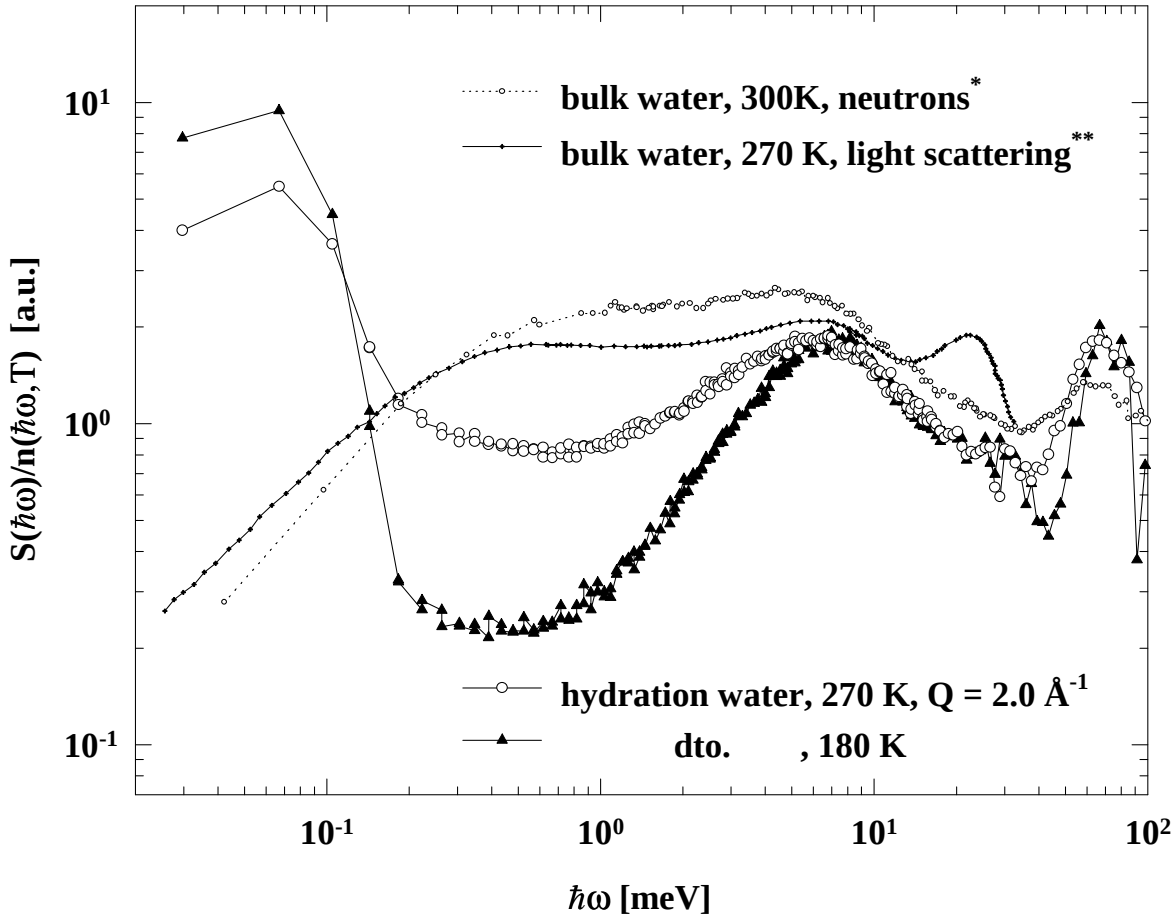
bulk water, 300K, neutrons*
bulk water, 270 K, light scattering**
hydration water, 270 K, Q = 2.0 Å-1
dto. , 180 K
S(ħω)/n(ħω,T) [a.u.]
ħω [meV]
10-1
100
101
102

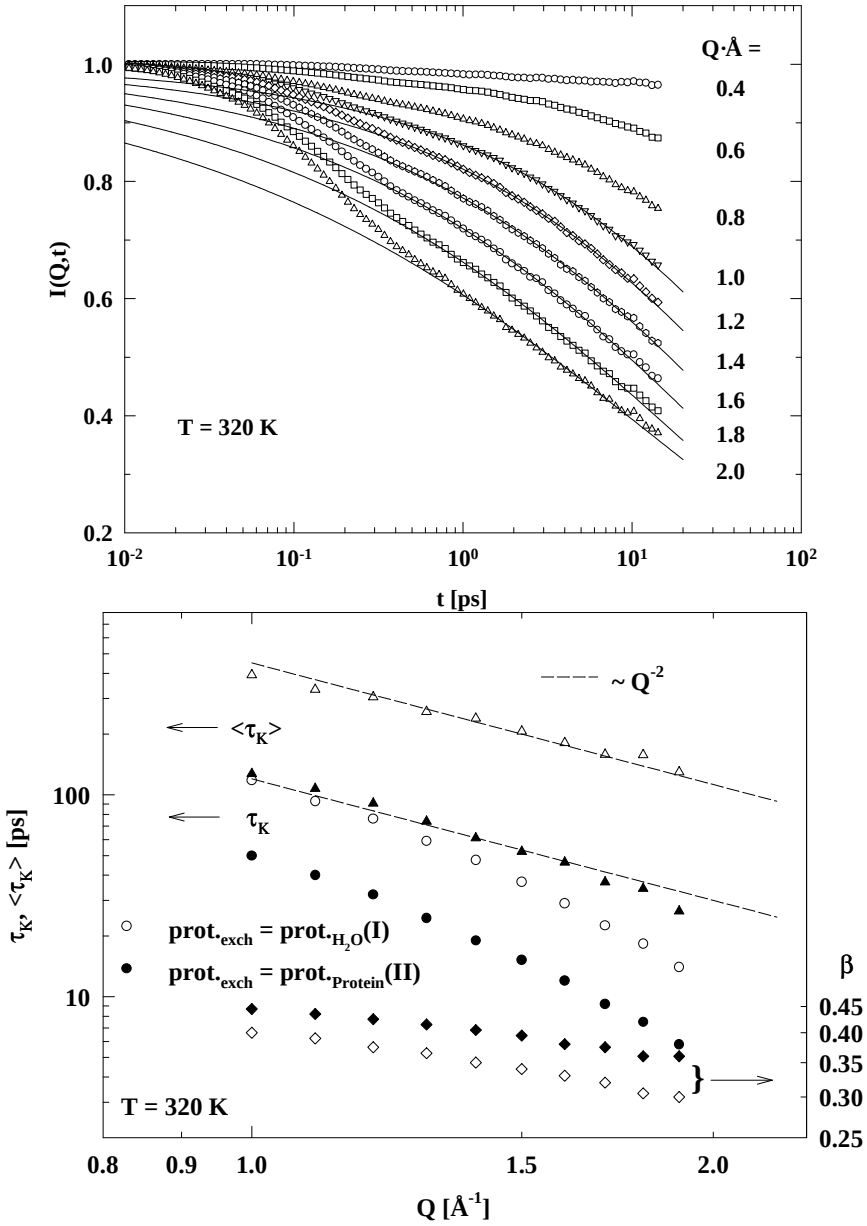
Q·Å =
0.4
0.6
0.8
1.0
1.2
1.4
1.6
1.8
2.0
I(Q,t)
T = 320 K
t [ps]
~ Q^-2
<τ_K>
τ_K
prot._exch = prot._H2O(I)
prot._exch = prot._Protein(II)
β
T = 320 K
τ_K, <τ_K> [ps]
Q [Å^-1]

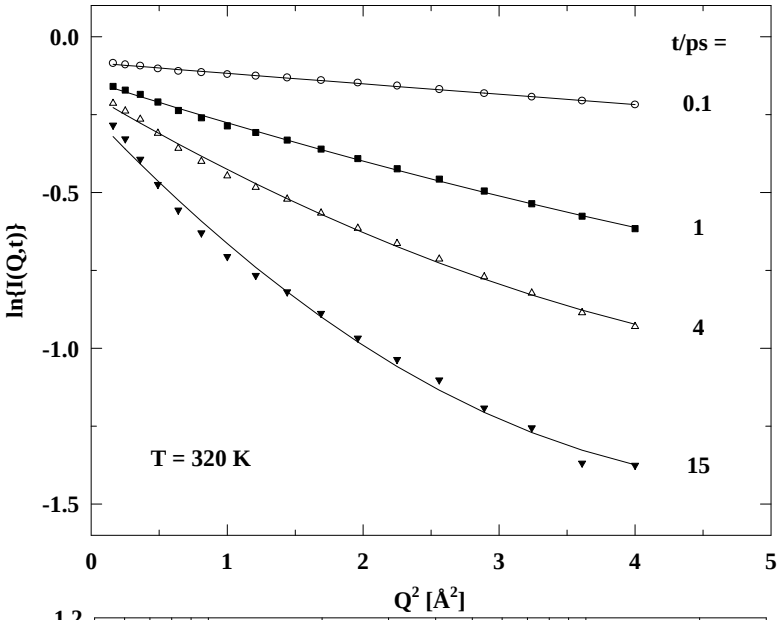
0.0
-0.5
-1.0
-1.5
ln{I(Q,t)}
t/ps =
0.1
1
4
15
T = 320 K
0
1
2
3
4
5
Q² [Å²]

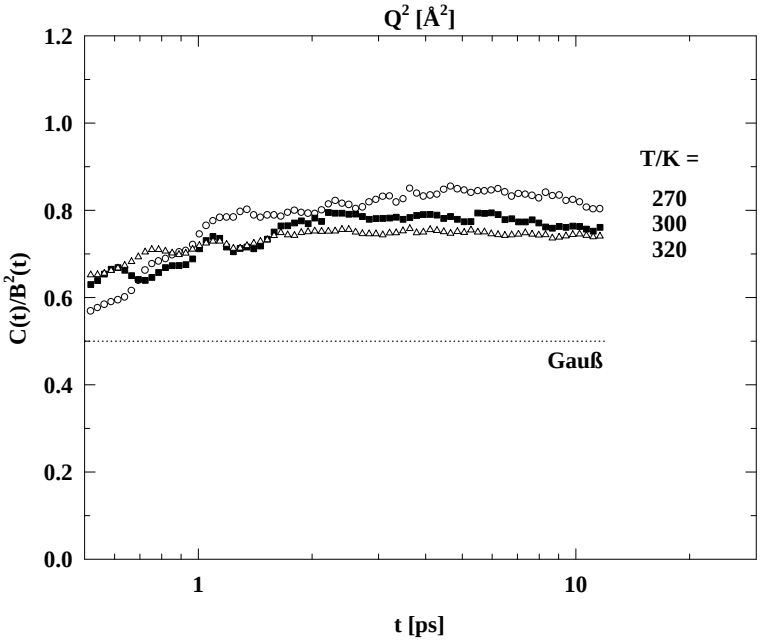
1.2
1.0
0.8
0.6
0.4
0.2
0.0
C(t)/B²(t)
T/K =
270
300
320
Gauß
1
10
t [ps]

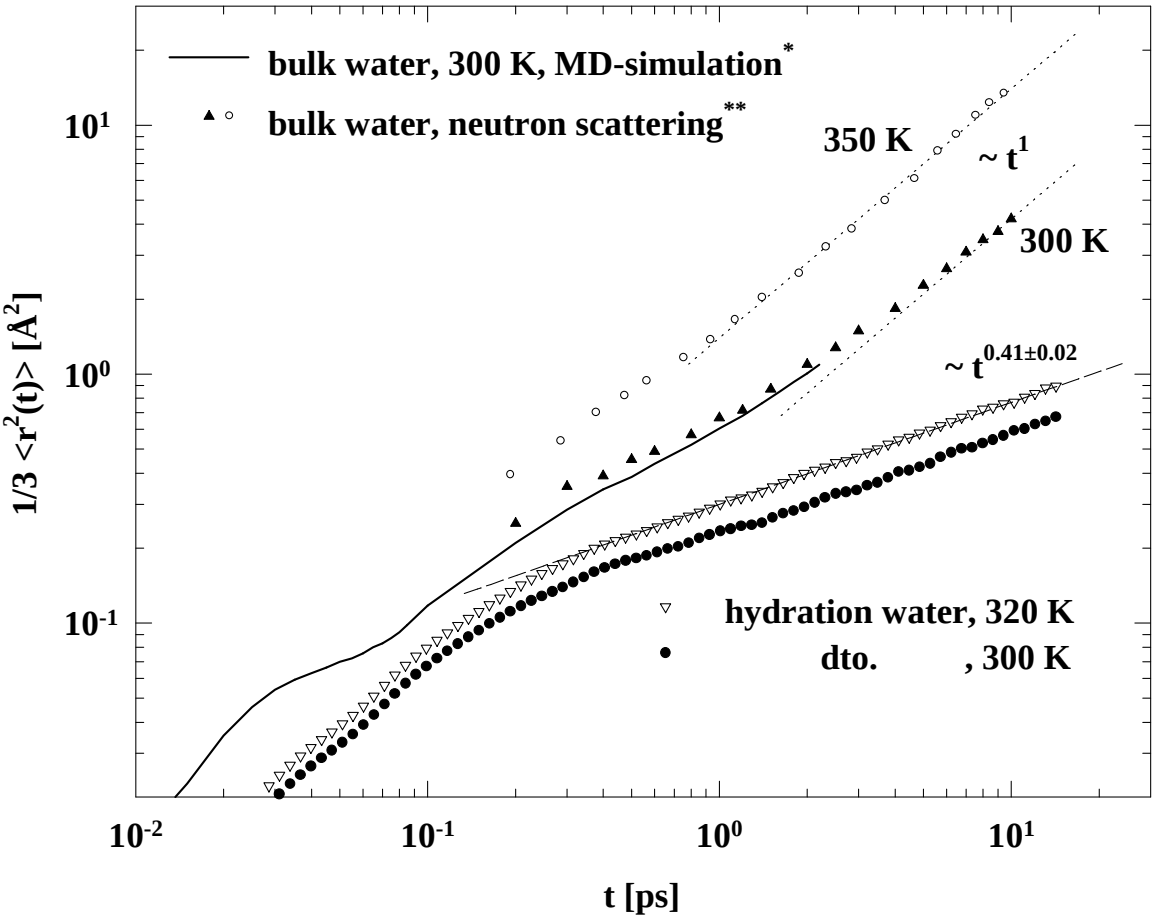
bulk water, 300 K, MD-simulation*
bulk water, neutron scattering**
350 K
~ t1
300 K
~ t0.41±0.02
hydration water, 320 K
dto. , 300 K
1/3 <r2(t)> [Å2]
t [ps]
10-2
10-1
100
101

References

[1] W. Doster, A. Bachleitner, R. Dunau, M. Hiebl, and E. Lüscher. Low temperature properties of water in myoglobin crystals and solutions. *Biophys. J.*, 50:213–219, 1986.

[2] G. Sartor, A. Hallbrucker, K. Hofer, and E. Mayer. Calorimetric glass-liquid transition and crystallization behaviour of a vitreous, but freezable water fraction in hydrated methemoglobin. *J. Phys. Chem.*, 96:5133–5138, 1992.

[3] H. E. Stanley and J. Teixera. *J. Chem. Phys.*, 73:3404, 1980.

[4] V. Lounas and B. M. Pettit. A connected cluster of hydration around myoglobin. *Proteins*, 18:133–147, 1994.

[5] R. Pethig. Protein-water interactions determined by dielectric methods. *Annu. Rev. Phys. Chem.*, 43:177–205, 1992.

[6] H. J. Steinhoff, B. Kramm, G. Hess, C. Owerdiek, and A. Redhardt. Rotational and translational water diffusion in the hemoglobin hydration shell. *Biophys. J.*, 65:1486–1495, 1993.

[7] M. G. Usha and R. J. Witteborg. Orientational ordering and dynamics of the hydrate and exchangeable hydrogen atoms in crystalline crambin. *J. Mol. Biol.*, pages 669–678, 1989.

[8] S. König, E. Sackmann, D. Richter, R. Zorn, C. Carlile, and T. M. Bayerl. Molecular dynamics of water in oriented DPPC multilayers. *J. Chem. Phys*, 100:3307, 1994.

[9] G. Otting, E. Liepinsh, and K. Wüthrich. Protein hydration in aqueous solution . *Science*, 254:974–980, 1991.

[10] J. Smith, K. Kuczera, and M. Karplus. *Proc. Natl. Acad. Sci. USA*, 87:1601–1605, 1990.

[11] P. J. Steinbach, A. Ansari, J. Berendzen, D. Braunstein, K. Chu, B. R. Cowen, D. Ehrenstein, H. Frauenfelder, J. B. Johnson, D. C. Lamb, S. Luck, J. R. Mourant, G. U. Nienhaus, P. Ormos, R. Philipp, A. Xie,

and R. D. Young. Ligand binding to heme proteins: connection between dynamics and function. *Biochemistry*, 30:3988–4001, 1991.

[12] C. X. Wang, A. R. Bizzari, Y. W. Xu, and S. Cannistraro. Molecular dynamics of copper plastocyanin. *Chem. Phys.*, 183:155–156, 1994.

[13] W. Doster, S. Cusack, and W. Petry. Dynamic transition of myoglobin revealed by inelastic neutron scattering. *Nature*, 337:754–756, 1989.

[14] W. Doster, S. Cusack, M. Settles, and F. Post. Hydration effects on protein function: Low frequency modes of partially hydrated proteins. In M. U. Palma, M. B. Palma-Vittorelli, and F. Parak, editors, *Water–Biomolecule Interactions Conf. Proc. vol. 43*, pages 127–130. SIF, Bologna, 1993.

[15] F. Parak, J. Heidemeier, and G. U. Nienhaus. Protein Structural Dynamics as determined by Mössbauer Spectroscopy. *Hyperfine Interactions*, 40:147–158, 1988.

[16] P. J. Steinbach and B. Brooks. Protein hydration eludicated by molecular dynamics simulation. *Proc. Natl. Acad. Sci. USA*, 90:9135–9139, 1993.

[17] M. C. Bellissent-Funel, J. Teixera, K. F. Bradley, and S. H. Chen. Dynamics of hydration water in protein. *J. Phys. I France*, 2:955–1001, 1992.

[18] R. E. Lechner, N. A. Dencher, J. Fitter, G. Büldt, and A. V. Belushkin. Proton diffusion on purple membrane studied by neutron scattering. *Biophys. Chem.*, 49:91–99, 1994.

[19] R. E. Lechner, N. A. Dencher, J. Fitter, and T. Dippel. Two dimensional proton diffusion on purple membrane. *Solid State Ionics*, 70/71:296–304, 1994.

[20] J. Teixeira, M. C. Bellissent-Funel, S. H. Chen, and A. J. Dianoux. *Phys. Rev. A*, 31:1913, 1985.

[21] J. Teixeira, M. C. Bellissent-Funel, and S. H. Chen. Dynamics of water studied by neutron scattering. *J. Phys. Condens. Matter*, 2:SA105–108, 1990.

[22] M. C. Bellissent-Funel, J. Teixera, K. F. Bradley, S. H. Chen, and H. L. Crespi. Single-particle dynamics of hydration water in protein. *Physica B*, 1992:740–744, 1992.

[23] M. Sakamoto, B. N. Brockhouse, R. G. Johnson, and N. K. Pope. Neutron inelastic scattering study of water. *J. Phys. Soc. Jap.*, 17:370–373, 1962.

[24] A. P. Sokolov, J. Hurst, and D. Quitmann. Dynamics of supercooled water: mode-coupling theory approach. *Phys. Rev. B*, 51,18:12 865, 1995.

[25] G. C. Lie and E. Clementi. Molecular dynamics simulation of liquid water. *Phys. Rev. A*, 33,4:2679, 1986.

[26] M. Fuchs, I. Hofacker, and A. Latz. Primary relaxation in a hard sphere system. *Phys. Rev. A*, 45,2:898, 1992.

[27] T. Kleinert, W. Doster, F. Post, and M. Settles. Hydration effects on protein function: The kinetics of ligand binding to myoglobin. In M. U. Palma, M. B. Palma-Vittorelli, and F. Parak, editors, *Water–Biomolecule Interactions Conf. Proc. vol. 43*, pages 127–130. SIF, Bologna, 1993.

[28] W. Doster, T. Kleinert, F. Post, and M. Settles. Effect of solvent on protein internal dynamics: The kinetics of ligand binding to myoglobin. In R. B. Gregory, editor, *Protein–Solvent Interactions*, chapter 8, pages 375–384. Marcel Dekker, Inc., 1995.

[29] R. H. Austin, K. W. Beeson, L. Eisenstein, H. Frauenfelder, and I. C. Gunsalus. Dynamics of ligand binding to myoglobin. *Biochemistry*, 14:5355–5373, 1975.

[30] G. P. Singh, F. Parak, S. Hunklinger, and K. Dransfeld. Role of adsorbed water in the dynamics of metmyoglobin. *Phys. Rev. Lett.*, 47,9:685–688, 1981.

[31] Marcus Settles. *Die Zeitabhängigkeit und Geometrie intramolekularer Bewegung globuläre Proteine aus Neutronenstreudaten*. Thesis, Technische Universität München, 1996.

[32] M. Diehl. private communication.

[33] G. E. Walrafen, M. R. Fischer, M. S. Hokmabadi, and W. H. Yang. Temperature dependence of the low-and high- frequency Raman scattering from liquid water. *J. Chem. Phys.*, 85:6970–6981, 1986.

[34] O. F. Nielsen. Low frequency studies of interactions in liquids. *Annu. Rep. Prog. Chem. Sec C, Phys. Chem.*, 90:3–44, 1933.

[35] N. J. Tao, G. Li, X. Chen, W. M. Du, and H. Z. Cummins. Low frequency Raman-scattering study of the liquid-glass transition in aqueous lithium chloride solutions. *Phys. Rev. A*, 44,10:6665–6676, 1991.

[36] J. Wuttke, W. Petry, G. Coddens, and F. Fujara. Fast dynamics of glass–forming glycerol. *Phys. Rev. E*, 52,4:4026–4034, 1995.

[37] J. Yarwood. Experimental determination of correlation functions from infrared and raman spectra. In A. J. Barnes et al., editor, *Molecular Liquids*, pages 357–382. D. Reidel Pub. Com., 1984.

[38] W. Götze and L Sjögren. Relaxation processes in supercooled liquids. *Rep. Prog. Phys.*, 55:241–376, 1992.

[39] W. G"otze. ed J.P.j Hansen et al., North Holland. *Liquids, Freezing and the Glass Transition*, pages 287–503, 1991.

[40] M. Fuchs. Comment ion Universal Self-Diffusion and Subdiffusion in Colloids at Freezing. *Phys.Rev.Lett.*, 74:1490, 1995.

[41] W. Doster, S. Cusack, and W. Petry. Dynamic instability of liquidlike motions in a globular protein observed by inelastic neutron scattering. *Phys. Rev. Lett.*, 65:1080–1083, 1990.